Talanta 128 (2014) 69–74

Contents lists available at ScienceDirect

Talanta

journal homepage: www.elsevier.com/locate/talanta

A fluorescence ratiometric chemosensor for Fe^{3+} based on TBET and its application in living cells

Cuicui Wang [a], Di Zhang [a], Xiaoyan Huang [b], Peigang Ding [a], Zhenji Wang [b], Yufen Zhao [a,c], Yong Ye [a,c,*]

[a] Phosphorus Chemical Engineering Research Center of Henan Province, The College of Chemistry and Molecular Engineering, Zhengzhou University, Zhengzhou 450052, China
[b] School of Pharmaceutical Science, Zhengzhou University, Zhengzhou, China
[c] Key Laboratory of Bioorganic Phosphorus Chemistry & Chemical Biology (Ministry of Education), Department of Chemistry, Tsinghua University, Beijing 100084, China

ARTICLE INFO

Article history:
Received 22 January 2014
Received in revised form
24 March 2014
Accepted 29 March 2014
Available online 23 April 2014

Keywords:
Rhodamine
Naphthalimide
Fluorescent chemosensor
TBET
Fe^{3+}

ABSTRACT

Based on a through bond energy transfer (TBET) between rhodamine and naphthalimide fluorophores, a fluorescent ratiometric chemosensor **L** was designed and prepared for highly selective detection of Fe^{3+} in aqueous solution and in living EC109 cells. These significant changes in the fluorescence color could be used for naked-eye detection. The reversibility established the potential of the probe as chemosensor for Fe^{3+} detection.

1. Introduction

Recently, the design and development of chemosensors for sensing and recognition of environmentally and biologically important heavy and transition metal ions have attracted considerable attention of current researchers [1–4]. Among transition metal ions, iron is the most abundant essential trace element for both plants and animals. It plays an important role in enzyme catalysis, cellular metabolism, and as an oxygen carrier in hemoglobin and a cofactor in many enzymatic reactions involved in the mitochondrial respiratory chain [5–7]. Besides the beneficial effects, less iron in the body has been reported to be linked to diabetes, anemia, liver and kidney damages, and heart diseases [8]. Much effort has been focused on the development of fluorescent Fe^{3+} indicators, especially those that exhibit selective Fe^{3+}-amplified emission [9–12].

Most reported Fe^{3+} fluorescent probes were based on fluorescence intensity. Although turn-on probes were more sensitive due to the lack of background signal, a major limitation was that variations in the sample environment (pH, polarity, temperature, and so forth) might influence the fluorescence intensity measurements. Besides an internal charge transfer (ICT) mechanism using a single fluorophore to obtain ratiometric changes, the exploration of multifluorophores with energy donor–acceptor architectures can achieve large pseudo-Stokes shifts, meanwhile affording simultaneous recorded ratio signals of two emission intensities at different wavelengths, which can provide a built-in correction for the environmental effects. Forster Resonance Energy Transfer (FRET) is generally the most adopted methodology for addressing this issue. The efficiency of FRET is primarily controlled by the spectral overlap between the emission spectrum of the energy donor and the absorption spectrum of the energy acceptor. In contrast to the FRET system, the TBET system is not limited by such a kind of spectral overlap and exhibits high energy transfer efficiencies, fast energy transfer rates and large pseudo-Stokes shift [13]. Therefore, TBET system has attracted attention, and been applied in many fields, such as optical materials [14], photosynthetic models [15], biotechnology [16–18] and chemosensors. However, to the best of our knowledge, a few fluorescent probes for Hg^{2+} and Cu^{2+} are reported on TBET [19], but no probe for Fe^{3+} based rhodamine–naphthalimide conjugate on TBET is

* Corresponding author at: Phosphorus Chemical Engineering Research Center of Henan Province, The College of Chemistry and Molecular Engineering, Zhengzhou University, Zhengzhou 450052, China. Tel.: +86 371 677 67050.
E-mail address: yeyong03@tsinghua.org.cn (Y. Ye).

http://dx.doi.org/10.1016/j.talanta.2014.03.073
0039-9140/

reported at present. Thus, it is important to develop ratiometric fluorescent probes for Fe^{3+} with favorable chemical and spectroscopic properties suitable for the imaging of Fe^{3+} in living cells.

As the fluorescence of the naphthalimide moiety was often quenched probably due to the efficient photoinduced electron transfer (PET) from the amide of rhodamine to the naphthalimide fluorophore, these probes could not exhibit any ratiometric fluorescence for metal ion detection [19h]. To solve this problem, herein, we reported a ratiometric fluorescent chemosensor **L** for Fe^{3+} based on TBET, in which (4-morpholine)-1,8-naphthalide (energy donor) and rhodamine (energy acceptor) were linked by a rigid and conjugated spacer p-phenylenediamine. Fortunately, this connection efficiently prevented the fluorescence quenching of naphthalimide. In the absence of Fe^{3+}, the excited energy of the naphthalimide donor could not be transferred to the rhodamine acceptor, as the rhodamine acceptor was in the closed form. Thus, only the emission of the dye naphthalimide was observed. A Fe^{3+}-induced process could change the emission maximum of the system from 535 nm (the characteristic peak of naphthalimide) to 586 nm (the characteristic peak of rhodamine). This wavelength shift allowed highly selective ratiometric detection of Fe^{3+} both in methanol/water solution and in living cells.

2. Experimental

2.1. Apparatus reagents and chemicals

ESI mass spectra were acquired in positive ion mode using a HPLC Q-Tof HR-MS spectrometer (Waters Micromass), which used methanol as mobile phase. NMR spectra were measured on a Bruker DTX-400 spectrometer using $CDCl_3$ as solvent and tetramethylsilane ($SiMe_4$) as internal standards. Fluorescence spectra measurements were recorded with a Hitachi F-4500 spectrofluorometer. A Techcomp UV-8500 spectrophotometer (Shanghai, China) was used for absorption measurements. The melting points were determined by an X-4 microscopic melting point apparatus with a digital thermometer.

All the materials for synthesis were purchased from commercial suppliers. Solvents for chemical synthesis were purified according to standard procedures. The solutions of metal ions were prepared from their chloride salts except for $AgNO_3$. The metal ions were prepared as 10.00 mM in water solution. Double distilled water was used throughout the experiment.

2.2. Synthesis of **L**

Compound **2** was synthesized according to the literature [20]. Compound **L** was synthesized using a method similar to that recently reported [21]. The concrete method is described as follows.

A stirred solution of rhodamine B (0.07 g, 0.15 mmol) in 1,2-dichloroethane (10 mL) and phosphorus oxychloride (0.3 mL) was added dropwise over 5 min at room temperature. The solution was refluxed for 4 h. The solvent was cooled and evaporated at reduced pressure to give rhodamine B acid chloride, which was impure and used in the next step directly. The crude acid chloride was dissolved in dry dichloromethane (10 mL) and added dropwise over 1 h to a solution of compound **2** (0.06 g, 0.16 mmol) and TEA (10 mL) in dichloromethane (15 mL) in an ice-bath. Then the resultant solution was allowed to warm to room temperature under nitrogen atmosphere over 24 h. The dichloromethane solution was removed under reduced pressure and the residue left was dissolved in dichloromethane, extracted with water, and dried over anhydrous Na_2SO_4. The organic layer was evaporated and the crude product was purified by column chromatography on silica gel using CH_2Cl_2/MeOH (20:1, v/v) as eluent to give **L** as yellow solid (64 mg, 53%). ^1H NMR ($CDCl_3$, 400 MHz, ppm): 1.18 (t, 12H, J=7.0 Hz), 3.29 (t, 4H, J=4.4 Hz), 3.34 (q, 8H), 4.04 (t, 4H, J=4.3 Hz), 6.30 (q, 2H, J=3.7 Hz), 6.36 (d, 2H, J=2.4 Hz), 6.70 (d, 2H, J=8.8 Hz), 7.11 (q, 3H, J=4.9 Hz), 7.25 (d, 1H, J=8.0 Hz), 7.39 (d, 2H, J=8.8 Hz), 7.49 (m, 2H), 7.72 (q, 1H), 8.02 (q, 1H), 8.46 (d, 1H, J=7.8 Hz), 8.52 (d, 1H, J=8.1 Hz), 8.57 (d, 1H, J=6.8 Hz); ^{13}C NMR ($CDCl_3$, 100 MHz, ppm): 12.65, 44.30, 53.43, 66.96, 98.03, 106.34, 108.26, 115.03, 117.19, 123.37, 123.46, 123.72, 125.84, 125.90, 126.22, 127.99, 128.50, 128.68, 129.71, 130.19, 130.30, 131.49, 132.50, 132.83, 133.07, 137.28, 148.82, 152.76, 154.11, 155.82, 163.92, 164.39, 168.26; HRMS calcd. for $C_{50}H_{47}N_5O_5$ $[M+H]^+$: 798.3650, found 798.3654; MP: 186–188 °C.

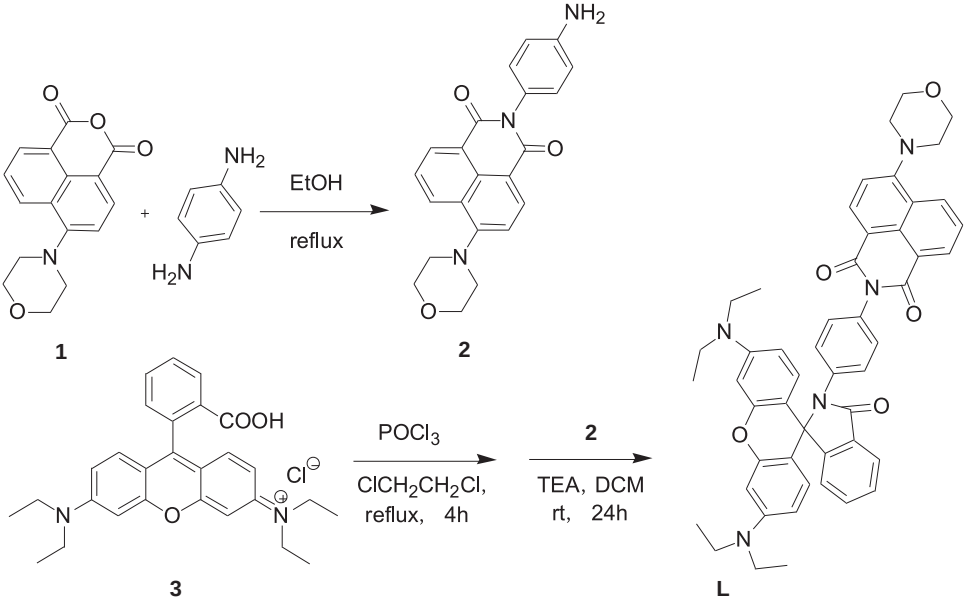

Scheme 1. Synthetic route of TBET-based ratiometric fluorescent Fe^{3+} chemosensor.

3. Results and discussion

3.1. Synthesis

As shown in Scheme 1, the probe **L** was synthesized by two steps. Firstly, compound **2** was obtained from 4-morpholin-1,8-naphthalic anhydride and p-phenylenediamine refluxed in ethanol. Rhodamine B acid chloride was synthesized by treating rhodamine B with $POCl_3$, and it was employed for the next reaction without further purification. Then the reaction between compound **2** and rhodamine B acid chloride was completed in dichloromethane and compound **L** gave 53% yield. All the new intermediates and compound **L** were well characterized by ^1H NMR, ^{13}C NMR, and HR-MS (Figs. S1–S3).

3.2. Fluorescence and absorbance spectra responses of **L**

The binding behaviors of compound **L** toward different cations were investigated by UV–vis and fluorescence spectroscopy. When no metal ion was added to the solution of **L**, only the absorption profile of the donor (1,8-naphthalimide) could be observed, which had a maximum at 406 nm (Fig. S4). A significant enhancement of the characteristic absorption of rhodamine B emerged at 562 nm soon after Fe^{3+} was injected into the solution. Such a large red-shift (156 nm) in absorption behavior changed the color of the solution from yellow to pink, allowing colorimetric detection of Fe^{3+} by the naked eye (Fig. 1 inset). And the lowest Fe^{3+} concentration was 18 μM (1.8 equivalent), which could be distinguished by the human eye (Fig. 2). Accordingly, as shown in Fig. 3, upon excitation at 420 nm, the free **L** displays a single emission band centered at 535 nm, which is attributed to the emission of the naphthalimide moiety. There was no TBET in the free **L**, as the rhodamine acceptor was in the ring-closed form. Addition of Fe^{3+} significantly decreased the fluorescence intensity around 535 nm, and simultaneously a new red-shifted emission band at around 586 nm gradually increased. These changes in the fluorescence spectrum stopped when the amount of added Fe^{3+} reached 10 equivalents of the probe. This means that the TBET process took place between the two fluorophores.

Under the identical condition, no obvious response could be observed upon the addition of other ions, including Zn^{2+}, Mg^{2+}, Ca^{2+}, Cd^{2+}, Pb^{2+}, Cu^{2+}, Hg^{2+}, Ba^{2+}, Ni^{2+}, Cr^{3+}, K^+, Ag^+, Co^{2+}, Fe^{2+}, Mn^{2+}, Na^+ and Li^+. Fig. 1 shows a large enhancement factor (20-fold) of absorbance at λ_{max}=562 nm upon the addition of 10 equivalents of Fe^{3+}. A mild increase of absorbance at 562 nm was also detected when the same amount of Cr^{3+} (causing 4-fold absorption enhancement) was added due to their low binding affinity to **L**. Other cations of interest gave no response. The results demonstrated that **L** was characteristic of high selectivity toward Fe^{3+} over other competitive metal ions.

Sensor **L** alone displayed a weak 1,8-naphthalimide emission band centered at 535 nm when excited at 420 nm (Fig. S5, excitation of 1,8-naphthalimide moiety). Upon addition of Fe^{3+}, the emission at 535 nm decreased, and a new emission band centered at 586 nm appeared with an isoemissive point. These changes could be ascribed to the Fe^{3+} induced opening of the spirocyclic ring of rhodamine moiety. The mode of energy transfer in receptor **L** was a very fast mechanism operating through bonds, i.e., via the conjugated linker which allowed energy transfer from donor to acceptor. However, the energy transfer was not 100% because some of the fluorescence leaked from the naphthalimide donor rather than being transferred to the acceptor. The emission intensities at 586 nm to that at 535 nm (F_{586}/F_{535}) are exhibited in Fig. S6. Sensor **L** (10 μM) exhibited a 30-fold enhancement of fluorescence intensity in the presence of 10 equivalents Fe^{3+}. A mild fluorescence enhancement factor (FEF) was also detected for Cr^{3+} (4-fold), and Zn^{2+}, Mn^{2+}, Mg^{2+}, Pb^{2+}, Ag^+, Cu^{2+}, Hg^{2+}, Co^{2+}, Ni^{2+}, Ca^{2+}, Ba^{2+}, Cd^{2+}, Li^+, Na^+, K^+, or Fe^{2+} showed nearly no response. Moreover, the studies of competitive metal ion binding and anion interference, which are carried out by adding

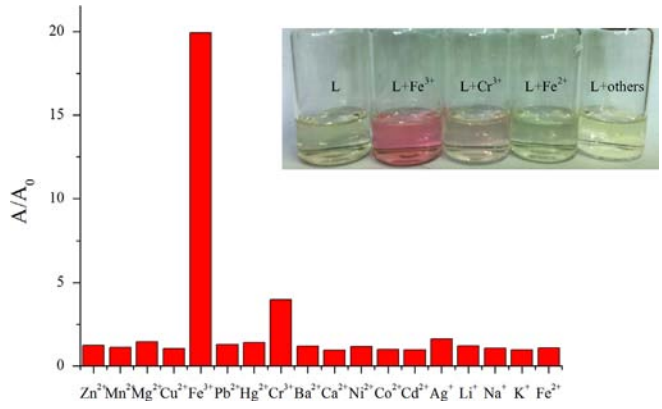

Fig. 1. Changes in the absorbance at 562 nm of **L** (10 μM) in the presence of 10 equivalents of various different metal ions in CH_3OH–H_2O (4:6, v/v) solution. Inset shows the photo of **L** with different metal ions. (For interpretation of the references to color in this figure, the reader is referred to the web version of this article.)

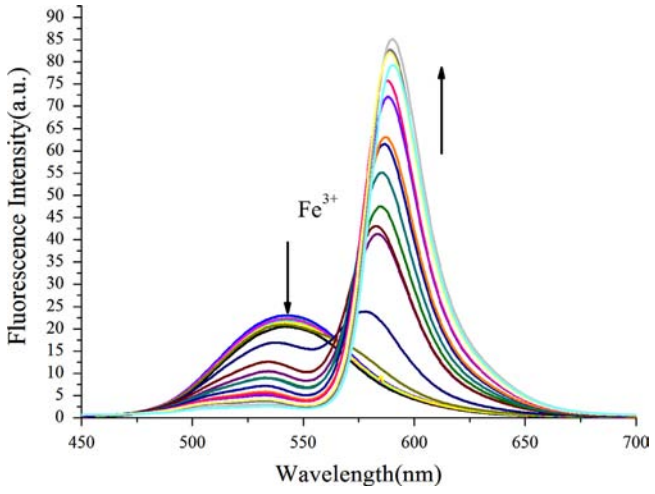

Fig. 3. Fluorescence ratio of **L** (80 μM) in response to the presence of Fe^{3+} (0–10 equivalents) in CH_3OH –H_2O (4:6, v/v) solution; λ_{ex}=420 nm.

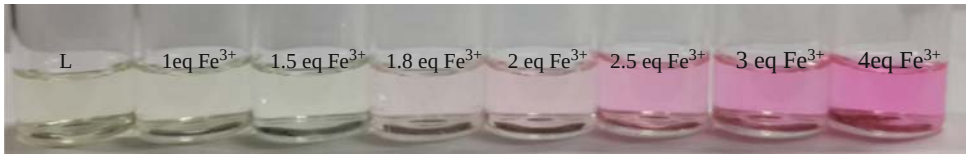

Fig. 2. Color changes in the presence of Fe^{3+} with different concentrations. [**L**]=10 μM. (For interpretation of the references to color in this figure legend, the reader is referred to the web version of this article.)

Fe^{3+} to **L** solution in the presence of other metal ions and anions as illustrated in Fig. 4 and Fig. S7, clearly establish the weak interference of other metal ions and anions on the Fe^{3+} fluorescence ratiometric detection by sensor **L**.

To determine the stoichiometry of the ferric–ligand complex, Job's method for absorbance measurement was applied. Keeping the sum of the initial concentration of Fe^{3+} and **L** at 100 μM, the molar ratio of Fe^{3+} was varied from 0 to 1. A plot of $[Fe^{3+}]/\{[Fe^{3+}]+[\mathbf{L}]\}$ versus the molar fraction of Fe^{3+} is provided in Fig. S8. It showed that the $Fe^{3+}/\{[Fe^{3+}]+[\mathbf{L}]\}$ value went through a maximum at a molar fraction of 0.5, indicating a 1:1 stoichiometry of Fe^{3+} to **L** in the complex. The binding constant (K) of **L** with Fe^{3+} ion was calculated according to the 1:1 model ($K = 1.24 \times 10^5$). Another direct evidence was obtained by comparing the ESI mass spectra of **L** and **L**–$FeCl_3$. As shown in Fig. 5; the cluster peak at m/z=959.0 (calculated 959.2) corresponding to $[\mathbf{L}+Fe^{3+}+3Cl^-+H^+]^+$ is clearly observed when 10 equivalents of $FeCl_3$ are added to **L**, whereas **L** without $FeCl_3$ exhibits peaks only at m/z=798.3, which correspond to $[\mathbf{L}+H^+]^+$. This indicated the formation of a 1:1 metal–ligand complex.

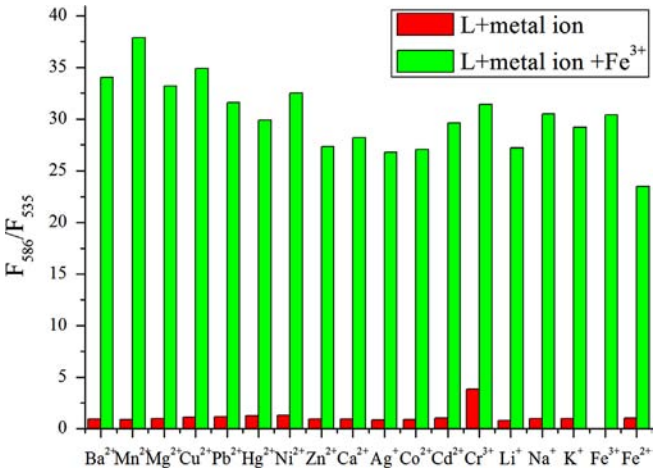

Fig. 4. Fluorescence responses of **L** to various cations in a CH_3OH –H_2O (4:6, v/v) solution. [**L**]=10 μM, $[M^{n+}]$=10 equivalents; λ_{ex}=420 nm; λ_{em}=586 nm.

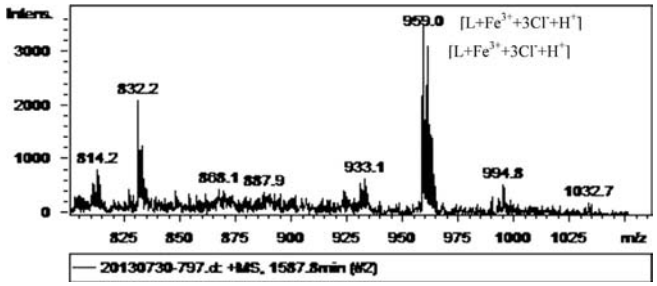

Fig. 5. ESI mass spectra (positive) of **L** in the presence of $FeCl_3$ (10 equivalents), indicating the formation of a 1:1 metal–ligand complex.

Generally, one of the most important and useful applications for a fluorescence sensor is the detection of metal ions. Under optimal conditions, the linear response for the fluorescence intensity response was between 0 and 20 μM (Fig. S9), and the detection limit of Fe^{3+} was measured to be 0.105 μM, which was lower compared with that of the sensor published in Scientific Journal of Environment Pollution and Protection [22] and was sufficiently low for the detection of sub-millimolar concentration ranges of Fe^{3+} ions in chemical and biological systems.

Further, it was of great interest to investigate the reversible binding nature of the sensor (shown in Fig. S10). To demonstrate the reversibility of **L**, K_3PO_4 (20 equivalents), as a strong affinity for Fe^{3+} was introduced into the solution containing **L** (10 μM) and Fe^{3+} (10 equivalents), the fluorescence intensity at 586 nm was decreased (green line) due to the competitive binding of Fe^{3+} from **L** by K_3PO_4 and further addition of 20 equivalents Fe^{3+} could recover the strong fluorescence again (blue line). This observation was assumed to be due to the decomplexation of Fe^{3+} by K_3PO_4 followed by a spirolactam ring closure reaction. Thus, a reversible fluorescent chemosensor for Fe^{3+} is constructed as shown in Scheme 2. We proposed that oxygen atom on the amide group participated in the chelation of Fe^{3+}.

Kumar reported a naphthalimide appended rhodamine derivative **1** through bond energy transfer for sensing of Hg^{2+} [19a]. Differences in the structures of compound **1** and **L** were connection sites of naphthalimide. Sensor **1** alone exhibited a very weak emission at 472 nm attributed to the naphthalimide moiety, and

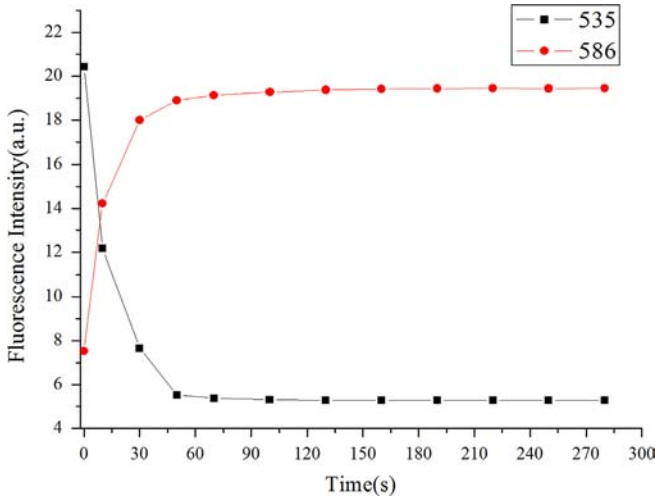

Fig. 6. Time-dependent fluorescence ratio (F_{586}/F_{535}) of **L** (10 μM) with Fe^{3+} (10 equivalents) in CH_3OH–H_2O (4:6, v/v) solution. Excitation wavelength is 420 nm.

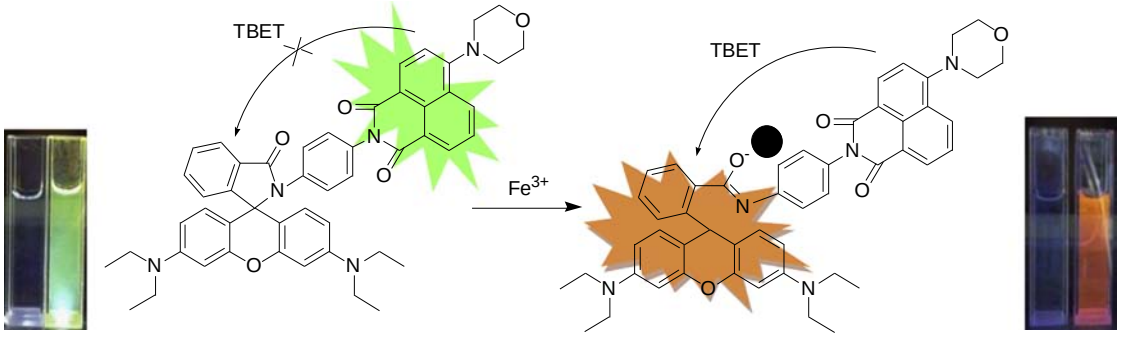

Scheme 2. Proposed mechanism of **L** with Fe^{3+}.

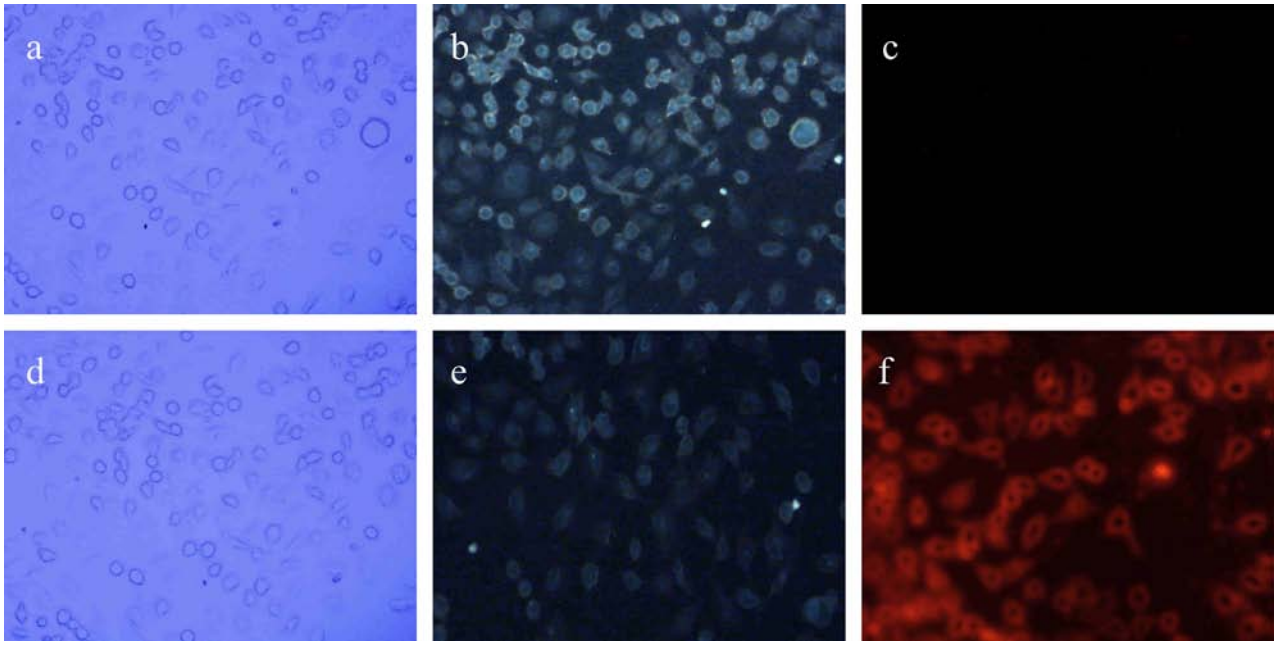

Fig. 7. Images of EC109 cells treated with the ratiometric **L**: (a) bright field image of EC109 cell incubated with **L** (5 μM); (b) fluorescence image from green channel; (c) fluorescence image from red channel; (d) bright field image of EC109 cell incubated with **L** (5 μM) for 15 min, and then further incubation with Fe^{3+} (5 μM) for 15 min at 37 °C; (e) fluorescence image from green channel; (f) fluorescence image from red channel.

the emission intensity was gradually increased after addition of Hg^{2+} (0–35 equivalents). The weak fluorescence emission of receptor **1** is due to the photoinduced electron transfer (PET) from nitrogen atom of the spirolactam ring to the photoexcited naphthalimide moiety. Compared with **1**, sensor **L** alone showed a strong emission at 535 nm (Fig. 3), as the photoinduced electron transfer (PET) was from nitrogen atom of 4-morpholin to the photoexcited naphthalimide moiety. Moreover, the emission intensity was gradually decreased upon addition of Fe^{3+} (0–10 equivalents). Therefore, compound **L** was used as a ratiometric fluorescent probe for Fe^{3+}.

To study the practical applicability, the fluorescence responses of sensor **L** in the absence and presence of Fe^{3+} at different pH values were evaluated (Fig. S11). The fluorescence titration curve of free sensor and **L**–Fe^{3+} showed the same enhancement between pH 1.0 and 3.0, but the fluorescence responses (F_{586}/F_{535}) of **L**–Fe^{3+} enhanced and free sensor decreased gradually afterwards, then both of them were not changed for pH values above 7.0, which meant that sensor **L** could work in near-neutral and weak acidic media.

Besides high selectivity, a short response time was one necessity for a fluorescent chemosensor to dynamically determinate Fe^{3+} in real-time. To study the response time of the chemosensor **L** to Fe^{3+}, the kinetics of fluorescence intensity at 535 nm and 586 nm by the new developed ratiometric fluorescent probe are recorded, and results are shown in Fig. 6. The time course of fluorescence intensity in the presence of Fe^{3+} indicated that stable reading could be obtained in less than 1 min, which had a shorter response time compared with that of RN1 towards Cu^{2+} as reported by Fan et al. [19h], so that it could be used as a fluorescent probe for the fast detection of Fe^{3+}.

3.3. *Bioimaging applications of compound **L** in EC109 cells*

Finally, due to the good chemical and spectroscopic properties of the probe, the ratiometric **L** was applied for ratiometric fluorescence imaging in living cells. When EC109 cells were incubated with only **L** (5 μM) for 15 min at 37 °C, these cells showed intense fluorescence in the green channel (Fig. 7b) and weak fluorescence in the red channel (Fig. 7c). However, treatment of Fe^{3+} (5 μM) with **L**-loaded cells elicited a partial fluorescence decrease in the green channel (Fig. 7e) and strong fluorescence in the red channel (Fig. 7f). Moreover, changes in the fluorescence intensity were researched with an increase of Fe^{3+} concentration (Fig. S12), which showed that Fe^{3+} detection limit was 1.25 μM in cells. These preliminary experimental results demonstrated that **L** could be used for detecting Fe^{3+} in biological samples.

4. Conclusions

In summary, we have designed and synthesized a new ratiometric fluorescent probe **L** for Fe^{3+} based on an intramolecular TBET. Sensor **L** has an excellent selectivity toward Fe^{3+} over other competitive metal ions, and allows spectrometric as well as naked-eye detection of Fe^{3+} levels in mixed aqueous solution, which provides a facile method for visual detection of Fe^{3+}. The main limitation of this probe is probably its moderate binding capacity to Fe^{3+} in aqueous media, but due to its excellent selectivity, the detection of Fe^{3+} at 0.105 μM level is still possible. The modification of **L** to develop new ratiometric fluorescent probes for Fe^{3+} with stronger binding ability is now under investigation.

Acknowledgments

This work was financially supported by the National Natural Science Foundation of China (Nos. 20972143 and 21375113) and Program for New Century Excellent Talents in University (NCET-11-0950).

Appendix A. Supporting information

Supplementary data associated with this article can be found in the online version at http://dx.doi.org/10.1016/j.talanta.2014.03.073.

References

[1] J.F. Callan, A.P. de Silva, D.C. Magri, Tetrahedron 61 (2005) 8551–8588.
[2] B. Valeur, I. Leray, Coord. Chem. Rev. 205 (2000) 3–40.
[3] L.J. Fan, Y. Zhang, C.B. Murphy, S.E. Angell, M.F.L. Parker, B.R. Flynn, Coord. Chem. Rev. 253 (2009) 410–422.
[4] A.P. de Silva, H.Q.N. Gunaratne, T. Gunnlaugsson, A.J.M. Huxley, C.P. McCoy, J. T. Rademacher, T.E. Rice, Chem. Rev. 97 (1997) 1515–1566.
[5] P. Aisen, M. Wessling-Resnick, E.A. Leibold, Curr. Opin. Chem. Biol. 3 (1999) 200–206.
[6] R. Meneghini, Free Radic. Biol. Med. 23 (1997) 783–790.
[7] R.S. Eisenstein, Annu. Rev. Nutr. 20 (2000) 627–662.
[8] C. Brugnara, Clin. Chem. 49 (2003) 1573–1578.
[9] H.N. Kim, M.H. Lee, H.J. Kim, J.S. Kim, J. Yoon, Chem. Soc. Rev. 37 (2008) 1465–1472.
[10] G.E. Tumambac, C.M. Rosencrance, C. Wolf, Tetrahedron 60 (2004) 11293–11297.
[11] Z.Q. Hu, Y.C. Feng, H.Q. Huang, L. Ding, X.M. Wang, C.S. Lin, C.P. Ma, Sensors Actuators B 156 (2011) 428–433.
[12] M. Beija, C.A.M. Afonso, J.M.G. Martinho, Chem. Soc. Rev. 38 (2009) 2410–2433.
[13] J.L. Fan, M.M. Hu, P. Zhan, X.J. Peng, Chem. Soc. Rev. 42 (2013) 29–43.
[14] (a) D.T. McQuade, A.E. Pullen, T.M. Swager, Chem. Rev. 100 (2000) 2537–2546; (b) J.M. Tour, Chem. Rev. 96 (1996) 537–554.
[15] D. Holten, D.F. Bocian, J.S. Lindsey, Acc. Chem. Res. 35 (2002) 57–62.
[16] G.S. Jiao, L.H. Thoresen, K. Burgess, J. Am. Chem. Soc. 125 (2003) 14668–14672.
[17] R. Bandichhor, A.D. Petrescu, A. Vespa, A.B. Kier, F. Schroeder, K. Burgess, J. Am. Chem. Soc. 128 (2006) 10688–10691.
[18] J.Y. Han, J. Jose, E. Mei, K. Burgess, Angew. Chem. Int. Ed. 46 (2007) 1684–1687.
[19] N. Kumar, V. Bhalla, M. Kumar, Analyst 139 (2014) 543–558;
(a) M. Kumar, N. Kumar, V. Bhalla, H. Singh, P.R. Sharma, T. Kaur, Org. Lett. 13 (2011) 1422–1425;
(b) P. Mahato, S. Saha, E. Suresh, R. Di Liddo, P.P. Parnigotto, M.T. Conconi, M.K. Kesharwani, B. Ganguly, A. Das, Inorg. Chem. 51 (2012) 1769–1777;
(c) V. Luxami, M. Verma, R. Rani, K. Paul, S. Kumar, Org. Biomol. Chem. 10 (2012) 8076–8081;
(d) V. Bhalla, V. Vij, R. Tejpal, G. Singh, M. Kumar, Dalton Trans. 42 (2013) 4456–4463;
(e) B. Yang, W. Wu, Anal. Methods 5 (2013) 4716–4722;
(f) V. Bhalla, M. Kumar, P.R. Sharma, T. Kaur, Inorg. Chem. 51 (2012) 2150-–2156;
(g) J.F. Zhang, Y. Zhou, J.Y. Yoon, Y.M. Kim, S.J. Kim, J.S. Kim, Org. Lett. 12 (2010) 3852–3855;
(h) J.L. Fan, P. Zhan, M.M. Hu, W. Sun, J.Z. Tang, J.Y. Wang, S.G. Sun, F.L. Song, X.J. Peng, Org. Lett. 15 (2013) 492–495.
[20] Y.L. Liu, X. Lv, Y. Zhao, M.L. Chen, J. Liu, P. Wang, W. Guo, Dyes Pigments 92 (2012) 909–915.
[21] C. Wu, Q.N. Bian, B.G. Zhang, X. Cai, S.D. Zhang, H. Zheng, S.Y. Yang, Y.B. Jiang, Org. Lett. 14 (2012) 4198–4201.
[22] C.W. Yu, J. Zhang, Sci. J. Environ. Pollut. Prot. 3 (2014) 1–7.